



Hydrothermal synthesis of Nb₂O₅-natural zeolite composite for enhanced adsorptive removal of anionic and cationic dye

Tarmizi Taher^{1,2}  Yohana Anastasya¹ Sephia Amanda Muhtar¹ Andika Munandar¹

¹ Department Engineering Physics, Faculty of Industrial Technology, Institut Teknologi Sumatera, Terusan Ryacudu, Way Hui, Jati Agung, Lampung Selatan 35365, Indonesia

² Center for Green and Sustainable Materials, Institut Teknologi Sumatera, Terusan Ryacudu, Way Hui, Jati Agung, Lampung Selatan 35365, Indonesia

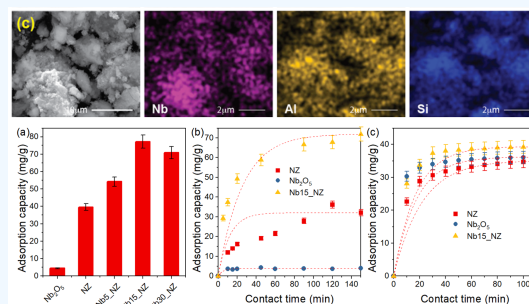
✉ Corresponding author: tarmizi.taher@tl.itera.ac.id

ARTICLE HISTORY: Received: December 1, 2024 | Revised: December 20, 2024 | Accepted: December 24, 2024

ABSTRACT

The imperative to mitigate dye pollution from wastewater has propelled the exploration of efficient adsorbents. This study deals with the preparation and evaluation of Nb₂O₅-supported natural zeolite NbX_NZ for enhanced dye adsorption performance. A facile hydrothermal method was employed to prepare NbX_NZ with varying niobium precursor loadings. Comprehensive material characterization employing FESEM, EDX, TGA, XRD, and FTIR analyses elucidate the successful incorporation of Nb₂O₅, revealing altered morphological and thermal properties. The adsorption test exhibited a notable augmentation in adsorption capacity for Congo red dye, particularly with the Nb15_NZ sample, showcasing a nearly two-fold increase compared to the parent natural zeolite. The findings underscore the potential of NbX_NZ as promising materials for anionic dye adsorption, paving the way for advancing wastewater treatment solutions and further investigations into metal oxide-modified zeolites.

Keywords: Niobium pentoxide, natural zeolite, adsorption, Congo red, Methylene blue



1. INTRODUCTION

Zeolites, owing to their high surface area, ion exchange capacities, and porous structure, have emerged as promising materials for adsorption applications [1, 2, 3]. One area that has garnered considerable attention is the adsorption of dyes from wastewater, a pervasive environmental issue accompanying the textile industry's growth [4, 5, 6]. However, the inherent limitations of natural zeolites, such as lower adsorption capacity for certain dyes, necessitate a modification to enhance their performance [7, 8]. Metal and nonmetal modification is a recognized strategy to augment the adsorption capabilities of zeolites [9, 10, 11, 12, 13, 14]. Among various metals, Niobium (Nb) stands out due to its unique properties. Nb, a transition metal, exhibits excellent chemical stability and a high affinity for a range of substances, making it a potential candidate for zeolite modification [15]. Additionally, Nb's ability to form stable complexes with organic molecules suggests a promising avenue for enhancing the adsorption of dyes on zeolite surfaces.

The impregnation of Nb into the natural zeolite framework aims to address the prevailing challenges. The hypothesis is that Nb modification would alter the zeolite's surface charge and pore structure, thereby increasing the surface area and the number of active sites available for dye adsorption. Furthermore, the interaction between Nb and dye molecules might facilitate a more effective adsorption process, mitigating the environmental impact of dye pollutants [10, 16]. This

study embarks on a systematic investigation into the preparation of Nb-modified natural zeolite and its subsequent evaluation of dye adsorption performance. Through a rigorous characterization and testing regimen, this work endeavors to elucidate the underlying mechanism driving the enhanced adsorption performance, proving a solid foundation for future and practical applications in wastewater treatment.

2. Experimental Section

2.1 Materials Preparation

Natural zeolite (clinoptilolite) sourced from PT. Paragon Perdana Mining served as the support for the synthesis of Nb₂O₅-containing adsorbent with varying niobium loading levels. Ammonium niobium oxalate (C₄H₄NNbO₉ xH₂O, Sigma-Aldrich, ANO) was employed as the niobium precursor. The materials were prepared by utilizing a facile hydrothermal method, with ANO loading of 5, 15, and 30 wt.%. Initially, 2 g of natural zeolite (NZ) was dispersed in 80 mL of distilled water and stirred for 15 min. This mixture was then subjected to ultrasonic dispersion for an additional 30 min to form a stable zeolite suspension. Following this, a specific amount of ANO was added to the zeolite suspension under vigorous stirring, and ultrasonic dispersion was maintained for the next 15 min. The resulting mixture was subsequently transferred to a Teflon-lined autoclave reactor and heated at 175 °C for 72 h. After the hydrothermal treatment, the obtained solid was collected using vacuum filtration and rinsed

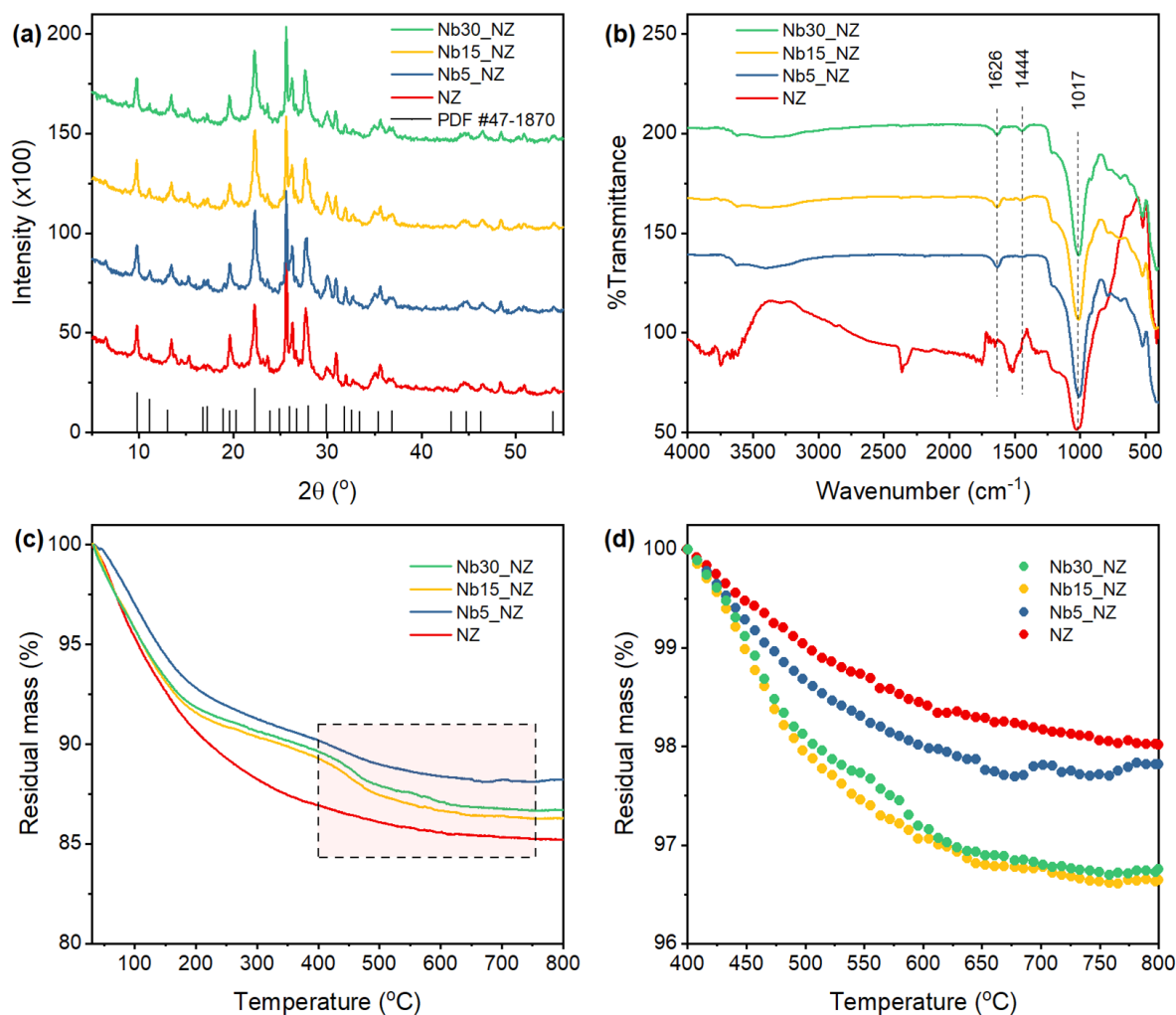


Figure 1. XRD pattern (a), FTIR spectra (b), TG curve (c), and TG curve at 400 – 800 °C (d), of the pristine natural zeolite and Nb₂O₅-supported zeolite

thrice with distilled water. The rinsed material was labeled as NbX_NZ, where X denotes the amount of ANO loaded, and NZ represents the natural zeolite.

2.2 Adsorption Study

The as-synthesized NbX_NZ was employed for the adsorption of both anionic (Congo red) and cationic (Methylene blue). The adsorption experiment was conducted in 250 mL conical flasks, each containing 100 mL of dye solution with a concentration of 50 mg/L and 0.05 g of the adsorbent. The flasks were agitated at 400 rpm at room temperature (25 – 30 °C). The effect of contact time was investigated by collecting samples at regular intervals (0 – 120 min) and analyzing the residual dye concentration using UV-Vis spectrophotometry. The adsorption capacity at equilibrium, q_e (mg/g), was calculated using the following Eq. (1).

$$q_e = \frac{(C_0 - C_e)}{mV} \quad (1)$$

Where C_0 and C_e are the initial and equilibrium concentrations of dye (mg/L), respectively, V is the volume of the solution (L), and m is the mass of the adsorbent (g).

3. RESULTS AND DISCUSSION

3.1 Materials Characterization

The X-ray diffraction (XRD) analysis was employed to scrutinize the crystalline structure and phase composition of both the NZ and NbX_NZ. Figure 1(a) shows the XRD pattern of these materials, where the characteristic peaks of clinoptilolite were identified and confirmed by JCPDS card number 47-1870. Interestingly, the XRD pattern of Nb₂O₅-supported zeolite demonstrated a resemblance to that of the pristine natural zeolite, which underscores the retention of the zeolite framework after niobium modification. This observation is in alignment with the findings of Ferreira et al., who reported analogous results when preparing Nb₂O₅-supported Y zeolite using the impregnation method [10]. They disclose that the preservation of the faujasite structure after Nb impregnation was confirmed by the comparable XRD pattern of the parent NaY zeolite and the Nb-modified samples.

Similarly, in our result, the similarity in the XRD pattern between the pristine and Nb₂O₅-modified zeolite substantiates the successful incorporation of Nb₂O₅ within the zeolite framework without altering its intrinsic structure. Moreover, no additional peaks corresponding to Nb₂O₅ were discerned in the XRD pattern of Nb₂O₅-supported zeolite, which might

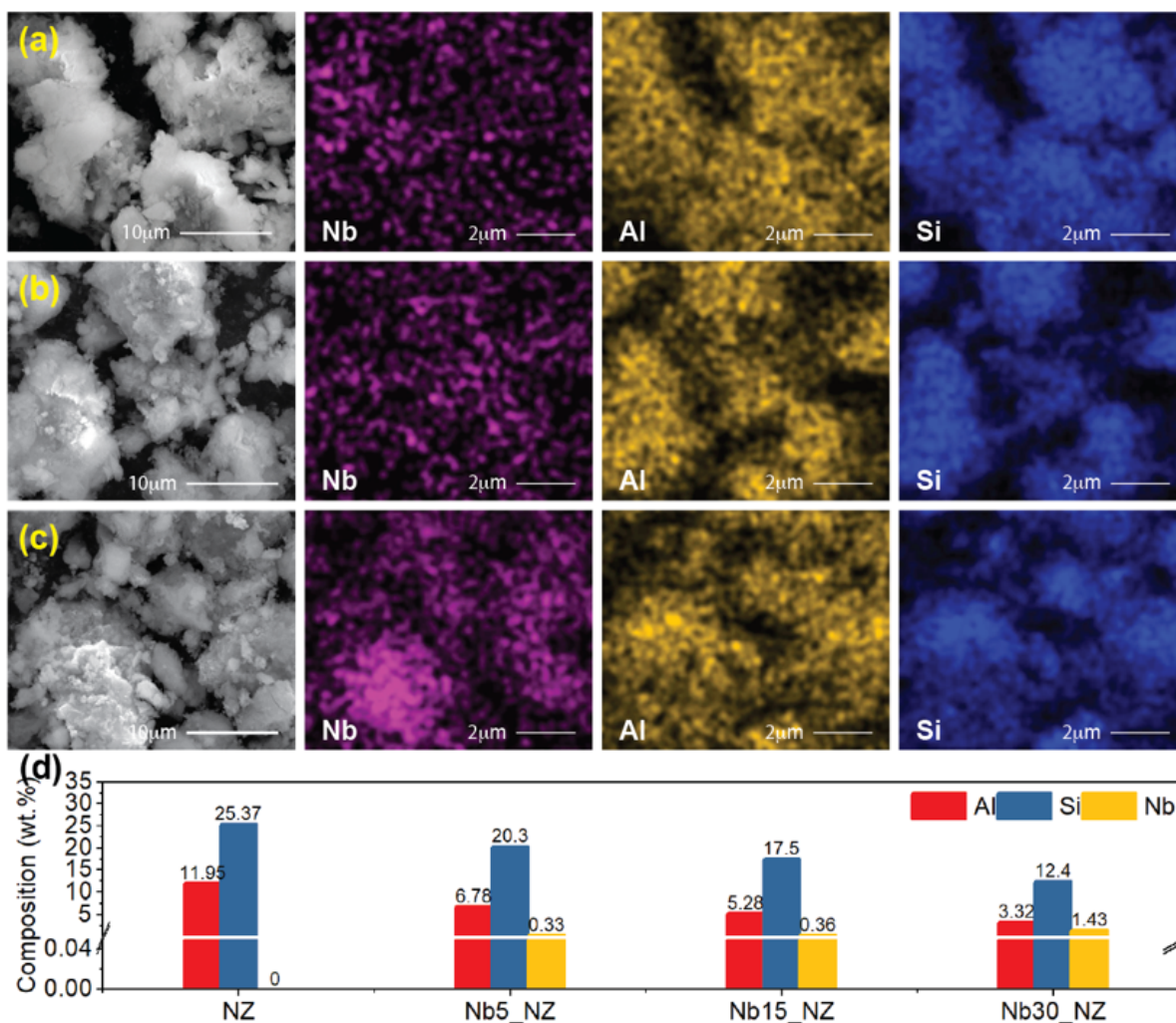


Figure 2. FESEM images and elemental mapping of (a) Nb5_NZ, (b) Nb15_NZ, (c) Nb30_NZ, and (d) atomic composition

suggest a well-dispersed state of Nb₂O₅ within the zeolite framework or potentially amorphous nature of Nb₂O₅ post-synthesis. Nb₂O₅ can exhibit several distinct phases based on various factors such as temperature and preparation methods. Based on our past studies on the preparation of Nb₂O₅ over a hydrothermal method using ANO precursor, it was reported that the obtained Nb₂O₅ exhibited an orthorhombic phase with a deformed structure [16]. However, the absence of crystalline structure of Nb₂O₅ in this study, as indicated by the XRD pattern, could be attributed to several factors. During the hydrothermal synthesis, the Nb₂O₅-support interaction can reduce the mobility of the niobium oxide species, making them more resistant to aggregation into crystalline phases. Moreover, this interaction can hinder the crystallization of Nb₂O₅, thereby preventing the formation of distinct crystalline phases [10].

The FTIR spectra of the prepared materials are presented in Figure 1(a). The acquired spectra both NZ and NbX_NZ, elucidate distinctive peaks at wavenumbers 3606, 3368, 1626, and 1017 cm⁻¹. The peaks observed at 3606 cm⁻¹ and 3368 cm⁻¹ are typically associated with the stretching vibration of hydroxyl (OH) groups [12]. These peaks could signify the presence of hydroxyl groups either internally within the zeolite framework or on its surface, affirming the hydrophilic nature of zeolite material. The peak at 1626 cm⁻¹ is sugges-

tive of bending vibration of molecular water (H₂O) entrapped within the zeolite pores or hydroxyl groups. While the most prominent peaks observed at 1017 cm⁻¹ is indicative of the asymmetric stretching vibration of Si-O or Al-O tetrahedral units within the zeolite framework [8] of the zeolite structure. Upon modification with niobium, a notable new peak emerged at 1444 cm⁻¹, which become more pronounced with increasing Nb loading. As inferred in our preceding work, the emergence of this peaks is postulated to signify the presence of ammonium ions within the pore structure of Nb₂O₅ [16]. Given the preparation of Nb₂O₅ from ammonium niobium oxalate precursor, it's plausible that the ammonium ions were retained within Nb₂O₅ post-synthesis.

The thermogravimetric (TGA) curve of the NbX_NZ and the zeolite support is presented in Figure 1(c). For NZ, it revealed a two-step decomposition pattern. A significant mass loss was observed from room temperature extending up to 400 °C, which could be attributed to the release of the physically adsorbed water, removal of hydroxyl groups, or the decomposition of any volatiles organic compound present [10]. Following this phase, a slower and more gradual mass loss was noted from 400 °C to 800 °C, possibly indicating the dehydroxylation process. Interestingly, the TGA curve of NbX_NZ unveils a more complex decomposition behavior in contrast to the pristine zeolite, manifesting three princi-

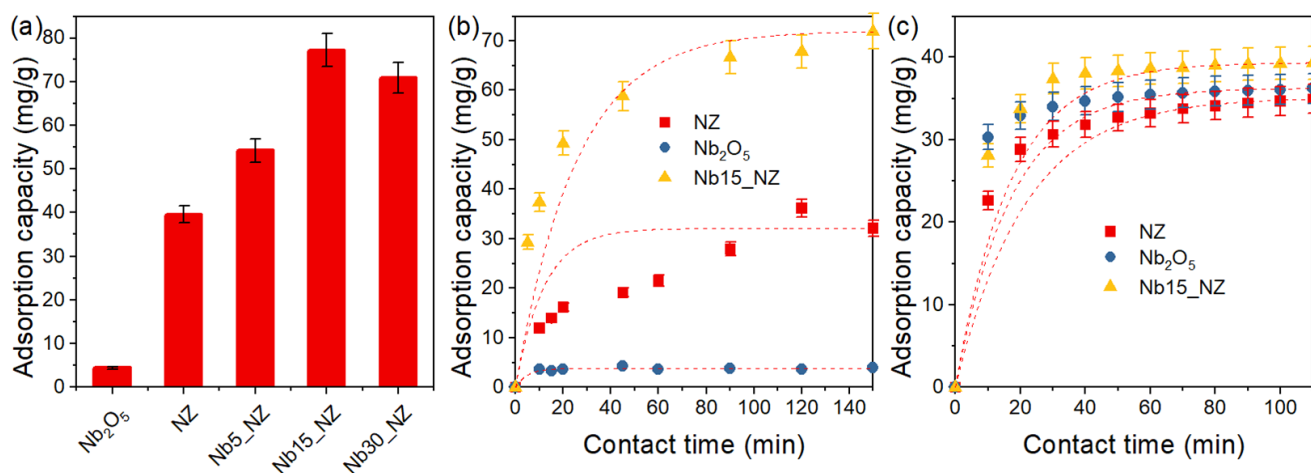


Figure 3. FESEM images and elemental mapping of (a) Nb₅_NZ, (b) Nb₁₅_NZ, (c) Nb₃₀_NZ, and (d) atomic composition

pal decomposition steps. These steps across the temperature ranges of room temperature to 200 °C, 200 to 400 °C, and 400 to 800 °C. Notably, the final step is markedly pronounced relative to the parent zeolite. As illustrated in Figure 1(d), the mass loss of NbX_NZ from 400 to 800 °C significantly surpass that of the parent natural zeolite. The calculated mass loss for NZ, Nb₅_NZ, Nb₁₅_NZ, and Nb₃₀_NZ within this decomposition temperature regime amounts to 1.72%, 1.97%, 3.00%, and 2.91% respectively, showcasing the influential role of niobium modification on the thermal decomposition characteristics of the zeolite. These findings further substantiate the successful incorporation of Nb₂O₅ onto the zeolite structure, a conclusion that align with the observation made in other studies.

Figure 2(a) – (c) displays the FESEM images of the niobium-doped natural zeolite with different ANO weight percentages prior to the hydrothermal process. All niobium-doped natural zeolite samples exhibit characteristics of particle agglomeration, revealing an irregular and somewhat clumped morphology, showing a common natural zeolite morphology. This appearance is accentuated by the rough texture of the particle surfaces, dotted with smaller crystallites potentially resulting from the doping process. The FESEM images are presented alongside the EDX elemental mapping of niobium (Nb), aluminum (Al), and silicon (Si) atoms. A significant amount of Al and Si atoms were observed for all samples (i.e., Nb₅_NZ, Nb₁₅_NZ, Nb₃₀_NZ). Interestingly, the Nb elemental mapping shows an increasing Nb atomic density, implying higher Nb percentages in the Nb₃₀_NZ sample compared to the other samples (Nb₅_NZ and Nb₁₅_NZ). These results are corroborated by the weight percentage (wt.%) elemental analysis of the samples depicted in Figure 2(d). It demonstrates that the Nb weight percentage increased from 0.33 wt.% to 1.43 wt.% from the Nb₅_NZ to Nb₃₀_NZ samples, confirming the increase in Nb composition on the nanocomposites with increasing ANO weight percentage prior to the hydrothermal process.

The adsorption capacity of the NZ and NbX_NZ for CR dye adsorption is depicted in Figure 3(a), calculated using Eq. (1), based on the changes in UV-Vis absorption intensity at 498 nm after 150 minutes of reaction time. The Nb₂O₅ sample was used as a control and exhibited very little adsorption capacity (below 5 mg/g) for CR dye. The NZ sample displayed an adsorption capacity of up to 40 mg/g, which increased

to 77 mg/g after adding 15wt.% of ANO (Nb₁₅_NZ) prior to the hydrothermal process. This represents nearly a 2-fold increase after adding niobium precursors. These findings indicate that the NbX_NZ have higher CR adsorption capabilities compared to the NZ samples. Moreover, Figures 3(b) and 3(c) depict the adsorption capacity over time of the control Nb₂O₅, unmodified natural zeolite, and niobium-doped natural zeolite against CR and methylene blue (MB) dyes, respectively. The addition of niobium significantly increased the adsorption capacity of the NZ sample for CR dyes, while no substantial increase in adsorption capacity for MB dyes was observed.

4. CONCLUSION

The preparation and characterization of Nb₂O₅-supported natural zeolite (NbX_NZ) highlighted its potential in enhancing adsorption performance. Nb₂O₅ incorporation significantly altered the zeolite's morphological and thermal properties. The adsorption test revealed a nearly two-fold increase in adsorption capacity for Congo red dye with Nb₁₅_NZ sample, marking an improvement from the parent natural zeolite. However, for methylene blue adsorption, it did not exhibit a substantial enhancement, indicating selective adsorption toward anionic dyes. These findings suggest that (NbX_NZ), particularly with 15 wt.% ANO loading, presents a promising material for anionic and cationic dye adsorption, addressing challenges associated with dye pollution.

ACKNOWLEDGEMENT

This research was supported in full by Kurita Asia Research Grant (22Pid18-U2) provided by Kurita Water and Environmental Foundation.

REFERENCES

- [1] E. Pérez-Botella, S. Valencia, F. Rey, *Zeolites in Adsorption Processes: State of the Art and Future Prospects*, Chemical Reviews 122 (24) (2022) 17647–17695. <https://doi.org/10.1021/acs.chemrev.2c00140>.
- [2] Y. Li, J. Yu, *Emerging applications of zeolites in catalysis, separation and host-guest assembly*, Nature Reviews Materials 6 (12) (2021) 1156–1174. <https://doi.org/10.1038/s41578-021-00347-3>.
- [3] T. Taher, E. K. A. Melati, M. Febrina, S. Maulana, M. A. Asagabaldan, A. Rianjanu, A. Lesbani, R. R. Mukti, *Effect of*

- Desilication on Indonesian Natural Zeolite for the Enhancement of Ammonium Ion Removal from Aqueous Solutions, *Silicon* 16 (3) (2024) 1309–1319. <https://doi.org/10.1007/s12633-023-02758-z>.
- [4] T. Shindhal, P. Rakholiya, S. Varjani, A. Pandey, H. H. Ngo, W. Guo, H. Y. Ng, M. J. Taherzadeh, *A critical review on advances in the practices and perspectives for the treatment of dye industry wastewater*, *Bioengineered* 12 (1) (2021) 70–87. <https://doi.org/10.1080/21655979.2020.1863034>.
- [5] H. Solayman, M. A. Hossen, A. Abd Aziz, N. Y. Yahya, K. H. Leong, L. C. Sim, M. U. Monir, K.-D. Zoh, *Performance evaluation of dye wastewater treatment technologies: A review*, *Journal of Environmental Chemical Engineering* 11 (3) (2023) 109610. <https://doi.org/10.1016/j.jece.2023.109610>.
- [6] M. D. Khan, A. Singh, M. Z. Khan, S. Tabraiz, J. Sheikh, *Current perspectives, recent advancements, and efficiencies of various dye-containing wastewater treatment technologies*, *Journal of Water Process Engineering* 53 (2023) 103579. <https://doi.org/10.1016/j.jwpe.2023.103579>.
- [7] Y. Zhou, J. Lu, Y. Zhou, Y. Liu, *Recent advances for dyes removal using novel adsorbents: A review*, *Environmental Pollution* 252 (2019) 352–365. <https://doi.org/10.1016/j.envpol.2019.05.072>.
- [8] A. Rianjanu, T. Taher, F. Desriani, R. O. Delmita, A. G. Sianturi, S. A. Muhtar, B. Ariwahjoedi, N. I. Khamidy, D. R. Adhika, M. F. Arif, *Examining the influence of sintering temperatures on the efficiency of 3D-printed natural zeolite for methylene blue dye adsorption*, *Results in Surfaces and Interfaces* 17 (2024) 100337. <https://doi.org/10.1016/j.rsufi.2024.100337>.
- [9] M. Popaliya, A. Mishra, *Modified zeolite as an adsorbent for dyes, drugs, and heavy metal removal: a review*, *International Journal of Environmental Science and Technology* 20 (11) (2023) 12919–12936. <https://doi.org/10.1007/s13762-022-04603-z>.
- [10] C. Ferreira, A. Araujo, V. Calvino-Casilda, M. Cutrufello, E. Rombi, A. Fonseca, M. Bañares, I. Neves, *Y zeolite-supported niobium pentoxide catalysts for the glycerol acetalization reaction*, *Microporous and Mesoporous Materials* 271 (2018) 243–251. <https://doi.org/10.1016/j.micromeso.2018.06.010>.
- [11] N. Zhu, M. Zhang, G. Qiu, H. Tian, Y. Liu, *One-pot synthesis of 5-hydroxymethylfurfural from cellobiose and sucrose using niobium-modified montmorillonite catalysts*, *Molecular Catalysis* 532 (2022) 112720. <https://doi.org/10.1016/j.mcat.2022.112720>.
- [12] S. Liu, Y. Ding, P. Li, K. Diao, X. Tan, F. Lei, Y. Zhan, Q. Li, B. Huang, Z. Huang, *Adsorption of the anionic dye Congo red from aqueous solution onto natural zeolites modified with N,N-dimethyl dehydroabietylamine oxide*, *Chemical Engineering Journal* 248 (2014) 135–144. <https://doi.org/10.1016/j.cej.2014.03.026>.
- [13] E. P. Favvas, C. G. Tsanaktsidis, A. A. Sapalidis, G. T. Tzilantonis, S. K. Papageorgiou, A. C. Mitropoulos, *Clinoptilolite, a natural zeolite material: Structural characterization and performance evaluation on its dehydration properties of hydrocarbon-based fuels*, *Microporous and Mesoporous Materials* 225 (2016) 385–391. <https://doi.org/10.1016/j.micromeso.2016.01.021>.
- [14] L. E. Burris, M. C. Juenger, *Effect of calcination on the reactivity of natural clinoptilolite zeolites used as supplementary cementitious materials*, *Construction and Building Materials* 258 (2020) 119988. <https://doi.org/10.1016/j.conbuildmat.2020.119988>.
- [15] C. Nico, T. Monteiro, M. Graça, *Niobium oxides and niobates physical properties: Review and prospects*, *Progress in Materials Science* 80 (2016) 1–37. <https://doi.org/10.1016/j.pmatsci.2016.02.001>.
- [16] T. Taher, A. Yoshida, A. Lesbani, I. Kurnia, G. Guan, A. Abudula, W. Ueda, *Adsorptive removal and photocatalytic decomposition of cationic dyes on niobium oxide with deformed orthorhombic structure*, *Journal of Hazardous Materials* 415 (2021) 125635. <https://doi.org/10.1016/j.jhazmat.2021.125635>.